applied sciences

MDPI

*Article*

# A Numerical Study of the Vibration Characteristics of a Haptic Actuator for a Dial Gear Shifter

**Joonsik Won [1], Kinyeong Ko [2], Heesoo Eom [2], Chulsook Kim [3], Jihyun Cho [3] and Howuk Kim [1,*]**

[1] Department of Mechanical Engineering, Inha University, 100 Inha-ro, Michuhol-gu, Incheon 22212, Republic of Korea
[2] R&D Center, LS Automotive Technologies Co., Ltd., Anyang-si 14067, Republic of Korea
[3] Advanced Research Group, Inha NNIZ Lab, Incheon 21315, Republic of Korea
* Correspondence: howuk@inha.ac.kr; Tel.: +82-32-860-7317

**Featured Application: Haptic actuator, human–machine interaction.**

**Abstract:** Human–machine interaction (HMI) is becoming increasingly important, especially in the automotive industry, where advancements in automated driving and driver assistance systems are key to enhancing driver safety and convenience. Among the many HMI interfaces, tactile sensing has been widely used in automotive applications as it enables instant and direct interactions with drivers. An area that remains underexplored among the tactile HMI interfaces is the application of haptic feedback to gear shifter modules. Therefore, this study investigates the design optimization of a dial gear shifter by analyzing the vibrations transmitted to the knob surface from an integrated haptic actuator. Specifically, we first tuned the mechanical properties of the haptic actuator (in terms of the resonance frequency and vibration level) in a simulation model by referring to experimental results. Next, a numerical model of a dial gear shifter was constructed, integrated with a haptic actuator, and tuned with the experimental results. The model was further optimized based on the design of the experiment and sensitivity analyses. The optimized design yielded a 24.5% improvement in the vibration level compared with the reference design, exceeding the minimum threshold (>~2.5 m/s$^2$ at 200 Hz) required for tactile sensing. The vibration enhancement (>22.x%) was also confirmed under the simulated hand-grabbing condition. This study is technically significant as it demonstrates that the haptic vibration in a dial gear shifter can be efficiently optimized through numerical analyses. This research will be used for the actual prototyping of a dial gear shifter to provide a safe driving experience for drivers.

**Keywords:** haptic actuator; finite element analysis; design optimization; dial gear shifter; transducer design; human–machine interaction

check for updates

**Citation:** Won, J.; Ko, K.; Eom, H.; Kim, C.; Cho, J.; Kim, H. A Numerical Study of the Vibration Characteristics of a Haptic Actuator for a Dial Gear Shifter. *Appl. Sci.* **2024**, *14*, 9242. https://doi.org/10.3390/app14209242

Academic Editor: César Vasques

Received: 12 September 2024
Revised: 4 October 2024
Accepted: 8 October 2024
Published: 11 October 2024

**Copyright:** © 2024 by the authors. Licensee MDPI, Basel, Switzerland. This article is an open access article distributed under the terms and conditions of the Creative Commons Attribution (CC BY) license (https://creativecommons.org/licenses/by/4.0/).

## 1. Introduction

Human–machine interaction (HMI) refers to the communication between humans and various machines, including cars, robots, and artificial intelligence [1]. In recent years, the role of HMI has become more significant, particularly in the automotive industry, owing to advancements in automated driving control and driver assistance systems [2,3]. Various interfaces exist to support the interactions between humans and machines. For example, graphical user interfaces (GUIs) enable interactions between computers and humans [4]. It is essential to install a GUI in modern cars for the driver to obtain information from the driving assistance system [5]. In addition to visual perception, humans and machines can interact through other senses, such as touch, hearing, and smell [6–8]. Consequently, future cars are predicted to adopt diverse hardware based on various sensory systems for improved HMIs.

Touch is an important human sense for perceiving the outer environment [9]. Haptics is a technology that provides tactile sensation feedback to users through vibration, force,

and pressure [10,11]. For example, haptic actuators are embedded in most mobile phones and can produce tactile feedback through which users recognize incoming calls or the arrival of important messages. In the automotive industry, the role of haptics has become increasingly important in various application fields because it can alter traditional feedback methods such as audio or vision. Audio feedback can be missed owing to the atmospheric noise that occurs while driving, and visual feedback can be missed while the driver concentrates on the outer driving environment. In contrast, haptic feedback can provide more effective attention to drivers under emergency conditions, such as impending collisions, unrecognized penetration into another driving lane, and unexpected jaywalkers [12,13]. A crucial technical advantage of haptics is that it can directly interact with human tactile sensations as long as the user touches a part of the machine. When driving a car, the driver must grip the steering wheel, place their feet on the pedals, and fasten the seatbelt while sitting on the car seat, all of which can play a role in the pass-through of haptic feedback [14–16]. Hence, haptics in cars can immediately and efficiently convey important information to drivers by using the vibration sensations of humans, which are less affected by the external environment.

For decades, several haptic assistance systems have been introduced in the automobile industry to ensure safe driving. Vibration stimulation on the dashboard can significantly reduce eyes-off-road time and decrease the potential for an accident while driving [17,18]. A steering wheel with haptic actuators can provide reference information to drivers for efficient steering movements while parking or while driving [19,20]. Haptics can aid in augmenting car safety by providing warnings during emergencies. For example, drivers can be made aware of potential collisions through tactile sensations [21]. Moreover, warning signals for sudden lane departures or violations of speed limits can be communicated via haptics [22]. Currently, many haptic technologies are commercially available, and HMI with haptics is no longer a new field.

Haptic actuators are typically installed on steering wheels, dashboards, seats, and pedals [23–26]. Despite the increasing importance of tactile sensing, haptic functions have rarely been considered for gear shifter modules. For example, inexperienced drivers could dangerously maneuver gear shifters, directly shifting from the 'D' (drive) to the 'R' (reverse or to the 'P' (park) mode. In traditional gear shifters, there are no physical warning tools for the driver to notice incorrect manipulation of the car. Moreover, the most recent design of a gear shifter transformed from a stick to a dial type in compact dimensions [27]. The disc-type gear shifter exhibited aesthetic superiority in addition to efficient use of space compared to traditional gear sticks. However, because the gear modes are controlled in a rotary manner, it increases the potential for a crude maneuver of the gear. Thus, considering the application of haptics to dial-type gear shifters is worthwhile for ensuring car safety as it alerts the driver of the incorrect manipulation of the gears.

This study aims to analyze the vibration levels in a dial-type gear shifter induced by a haptic actuator and deduce an optimal design for the actuator integration to deliver the most efficient level of tactile vibrations to users. The haptic actuator installed in the gear shifter used for the experiment was an electromagnetic linear resonant actuator (LRA). Although it has a very narrow frequency bandwidth, the LRA is known to produce a relatively high vibration output compared to the voltage input [28]. An efficient vibration output and a compact design are critical for the application of a dial gear-shifting module with a geometric size of approximately 8 cm. We hypothesized that the input vibrational force generated by the electromagnetic effect could be indirectly estimated by comparing the experiment and simulation results. Following the confirmation of the numerical model, the results of the finite element analysis (FEA) determined the optimal design of the gear shifter and predicted the vibration level at the gripping positions with the required voltage level in the haptic actuator. This study provides an efficient method for estimating the input force caused by the electromagnetic effect and presents a comprehensive evaluation of the design to validate the performance of the haptic device.

## 2. Materials and Methods

### *2.1. Structure of the Haptic Actuator*

The haptic actuator (Figure 1) comprised a housing structure, an electromagnetic system, a vibration system, and a damper. The vibration system consisted of a spring and a weight to convert the electromagnetic force derived from the electromagnetic system into kinetic energy. Specifically, the application of an electric current to the coil creates a magnetic field, making the yoke polar and causing the magnet to oscillate. Finally, the housing structure of the actuator was a metallic case, and a bracket protected the internal parts on the bottom side of the actuator.

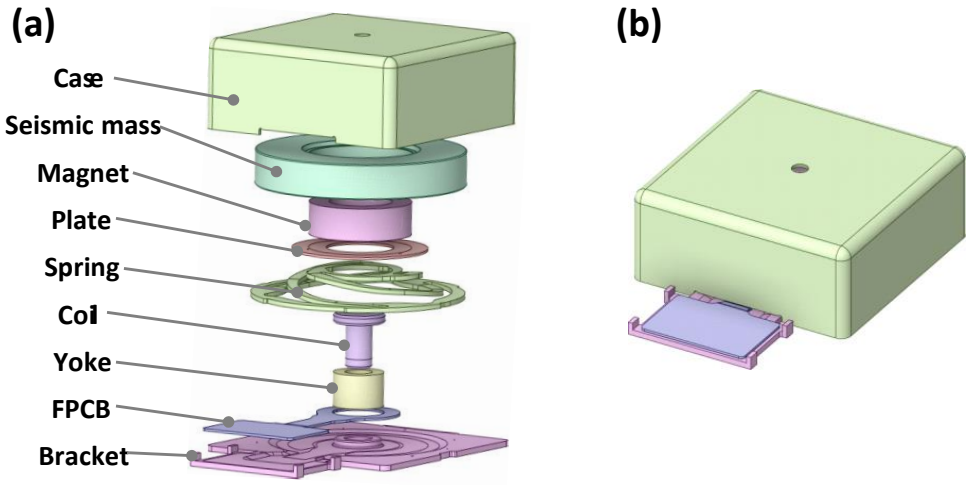


**Figure 1.** Structure of the haptic actuator in (**a**) the exploded view and (**b**) the assembly view.

### *2.2. Finite Element Analysis for Transducer Design*

Modal analysis is an important technique for analyzing and predicting the vibration characteristics of complex structures or systems. For a multi-degree of freedom (MDOF) system, the equation of motion for x(t) is written as

$$\mathbf{M}\ddot{\mathbf{x}} + \mathbf{C}\dot{\mathbf{x}} + \mathbf{K}\mathbf{x} = \mathbf{F}(t), \tag{1}$$

where **M**, **K**, and **C** denote the mass, stiffness, and damping matrices of the vibration system, respectively. $\mathbf{F}(t)$ is the excitation force in the MDOF system. For the harmonic forcing condition, the vibration output is determined as follows:

$$\mathbf{x}(\mathrm{t}) = \mathbf{X}(\omega)\sin(\omega t + \varphi), \tag{2}$$

where $\omega$ is the radial frequency, $\mathbf{X}(\omega)$ is the frequency response function, and $\varphi$ is the phase difference. Using modal analysis, the displacement for the k-th mode can be written as

$$\mathbf{x}_\mathrm{k}(\mathrm{t}) = \mathbf{X}_\mathrm{k}(\omega)\sin(\omega t + \varphi_\mathrm{k}), \tag{3}$$

The transfer function for the k-th mode, Hk($\omega$), characterizes how the vibrational response at a certain spatial point responds to harmonic excitation across a range of frequencies. It is a complex function of frequency, providing both magnitude and phase information, which is crucial for understanding the resonance behavior and dynamic characteristics of the system.

$$\mathbf{H}_\mathbf{k}(\omega) = \frac{\mathbf{X}_\mathrm{k}(\omega)}{\mathbf{F}_\mathrm{k}(\omega)}. \tag{4}$$

### 2.3. Electromagnetic Field Analysis of Haptic Actuator

We first computed the electromagnetic force, which was then used to estimate the excitation force of the haptic actuator. Theoretically, the electromagnetic force can be calculated as follows [29]:

$$F = \int J \times B dV, \tag{5}$$

where $J$ is the current density, $B$ the magnetic flux density, and $dV$ is the infinitesimal volume. The design parameters used to estimate the magnetic forces are listed in Table 1. The magnetic force mainly depends on the inner and outer diameters of the coil, number of windings, resistance of the coil, and applied voltage. The average magnetic flux density was simulated to be 0.58 T according to ANSYS Maxwell (rel. 2024, Canonsburg, PA, USA), and the magnetic force was computed to be 0.1003 N (Equation (5)).

**Table 1.** Design parameters of the electromagnetic coil.

| Inner Diameter (mm) | Outer Diameter (mm) | Number of Turns | Resistance (Ω) | Voltage (V) |
|---|---|---|---|---|
| 1.23 | 2.25 | 186 | 6 | 1 |

### 2.4. Simulation for the Haptic Actuator

Figure 2 shows the simulation model used to examine the vibration characteristics of the haptic actuator. The input force refers to the magnetic force estimated by the electromagnetic field analysis. A test jig with dimensions 105 mm × 45 mm × 15 mm was also incorporated into the simulation model to enhance the accuracy of the numerical analysis under actual testing conditions. A haptic actuator was attached to the upper surface of the jig at the position $x$ = 10 and $y$ = 22.5 mm. The vibration response was measured 9.5 mm from the actuator. Table 2 summarizes the material properties of the numerical simulation model.

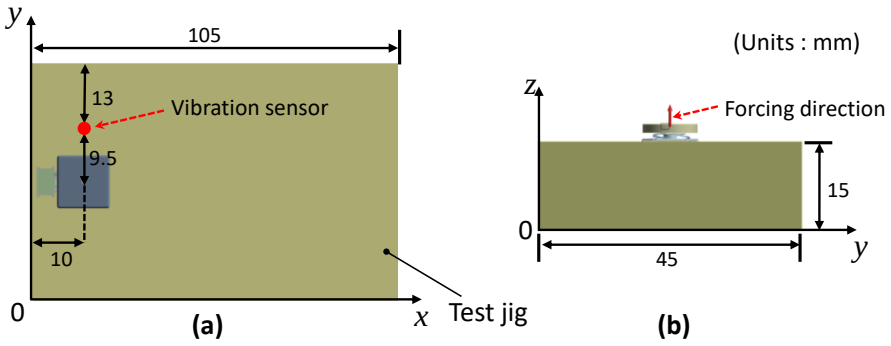


**Figure 2.** Geometry of the simulation model for the haptic actuator in (**a**) top-down view and (**b**) side view.

**Table 2.** Material properties of the simulation model.

| Part | Material | Density (kg/m$^3$) | Young's Modulus (GPa) | Poisson's Ratio |
|---|---|---|---|---|
| Bracket<br>Yoke<br>Case | SPCC | 7870 | 200 | 0.23 |
| Spring | SUS301 | 7800 | 190 | 0.3 |
| Weight | Tungsten | 19,500 | 411 | 0.28 |
| Magnet | Nd-Fe-B | 7600 | 150 | 0.24 |
| Jig | Bakelite | 1380 | 7.5 | 0.35 |

### 2.5. Vibration Tests of the Haptic Actuator

Figure 3 shows the test setup used to measure the vibration response of the haptic accelerator. The input over the actuator was given by a unit AC voltage. We measured the frequency response of the actuator by sweeping the excitation frequency from 170 to 220 Hz. The output acceleration was measured using an accelerometer attached at a distance of 9.5 mm from the actuator. The accelerometer signal was measured while the motor tester (BaKo 2120C, BaKo Co., Ltd., Suwon, Republic of Korea) operated the haptic actuator in frequency sweeping mode. The resonance frequency and maximum force of the developed haptic actuator were then determined using this test setup. The frequency response function measured by the actual haptic device was compared with the simulation results to ensure the forcing condition of the numerical model. Following the characterization of the haptic actuator, we introduced the forcing condition of the haptic device into the entire dial gear shifter model. Figure 4 shows the simulation process used in this study.

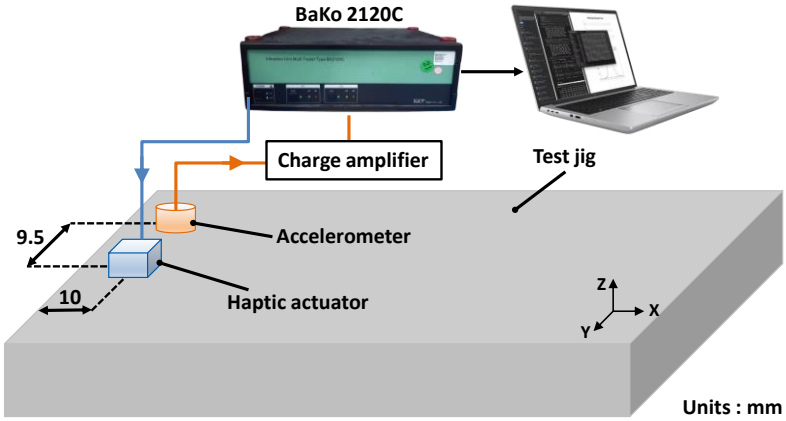


**Figure 3.** Test setup for characterizing the vibration response of the haptic actuator.

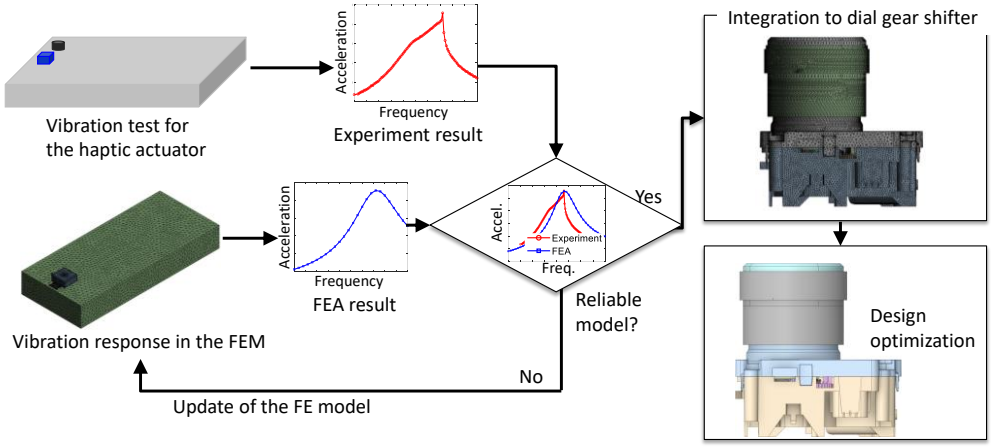


**Figure 4.** Overall simulation process to obtain the optimal design of the dial gear shifter.

### 2.6. Numerical Model of the Dial Gear Shifter

Figure 5 shows the FE model of the dial gear shifter and the relevant boundary conditions. The haptic actuator was integrated into the dial gear shifter, as shown in Figure 5. The forcing condition refers to the magnetic force generated by a haptic actuator. Because potential users generally manipulate a dial gear shifter by touching a cylindrical knob surface, the target vibration level was estimated from the knob surface by taking the average. First, the vibration level of the knob was computed using a baseline model. Next, design modifications were applied to the numerical model to further enhance the vibration output of the haptic actuator. Figure 6 shows some of the parameters addressed in the

design optimization process. The four design parameters were selected in the range of not having a significant effect on the functionality of the haptic module. For example, the geometric dimensions of the knob grip were modified. The influence of side supports was also assessed for the cavity in which the actuator was loaded. Furthermore, the knob grip was attached to the outer part (i.e., the fabrication method) using two different methods—bolting at four places and bonding over the surface. We followed the design optimization process for the dial gear shifter to achieve the highest level of vibration response. In this study, we utilized the Taguchi method, a well-known practical optimization tool [30]. The key to the Taguchi method is optimizing the signal-to-noise ratio (SNR), which is an indicator that quantifies the sensitivity of the system performance. We estimated the SNRs for each combination of design parameters using the following equation:

$$SNR = -10\log\left(\frac{1}{N}\sum_{i=1}^{N}\frac{1}{x_i^2}\right), \quad (6)$$

where $x_i$ is the output value of the i-th design parameter combination. Here, we modified four design parameters such that the L9 orthogonal array was used for the design of the experiment (Table 3).

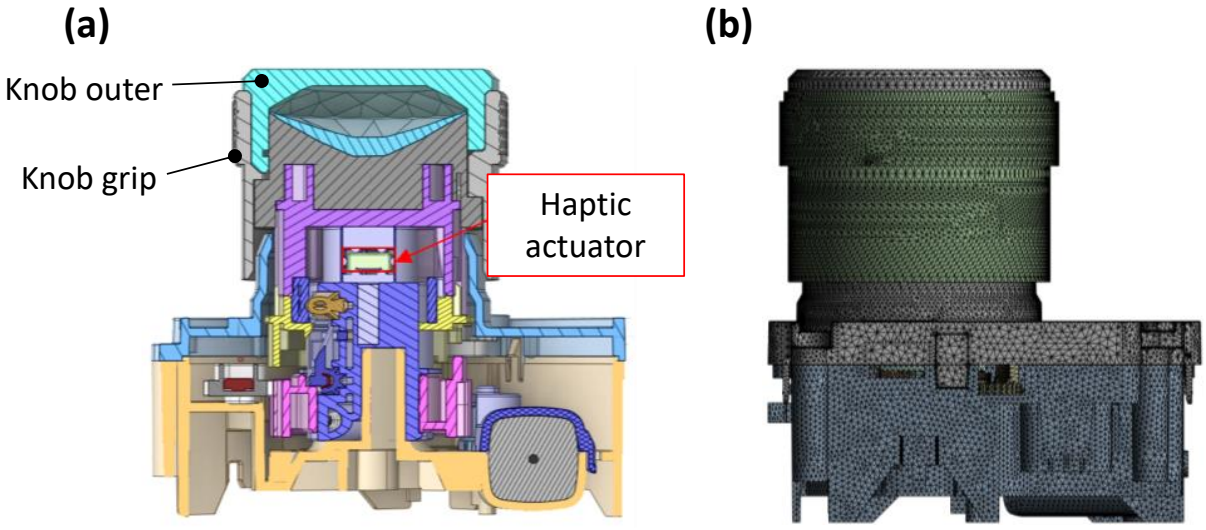


**Figure 5.** (**a**) Three-dimensional model of the dial gear shifter integrating the haptic actuator (i.e., the red solid box) and (**b**) the construction of the FE model.

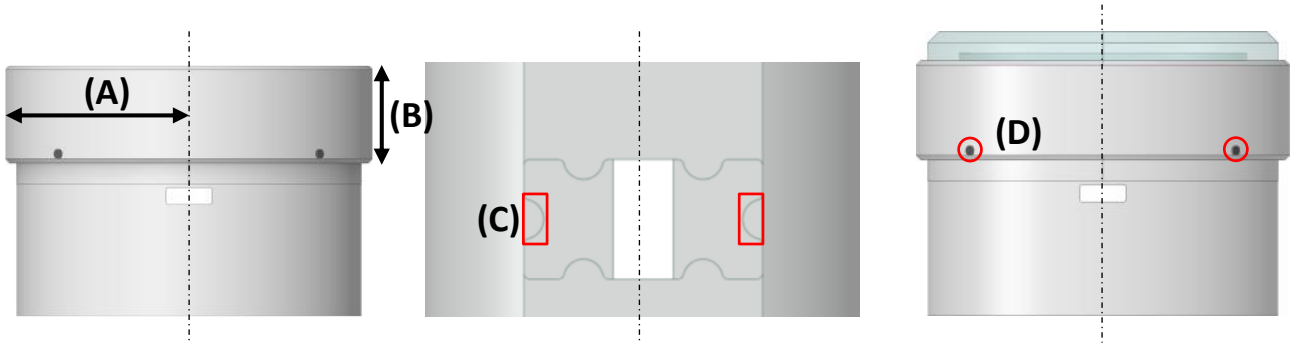


**Figure 6.** Design parameters to enhance the vibration response at the dial gear-shifting knob: (**A**) radius of knob grip, (**B**) longitudinal length of knob grip, (**C**) with and without the side supports in the cavity, and (**D**) attaching method between the knob grip and the knob outer part.

**Table 3.** Design of experiment (L9 orthogonal array).

| No. | (A) (mm) | (B) (mm) | (C) | (D) |
|---|---|---|---|---|
| 1 | 32 | 17 | 1 | 1 |
| 2 | 32 | 15.5 | 0 | 1 |
| 3 | 32 | 14 | 1 | 1 |
| 4 | 31 | 17 | 0 | 1 |
| 5 | 31 | 15.5 | 1 | 0 |
| 6 | 31 | 14 | 0 | 0 |
| 7 | 30 | 17 | 1 | 1 |
| 8 | 30 | 15.5 | 0 | 0 |
| 9 | 30 | 14 | 1 | 0 |

## 3. Results and Discussion

### *3.1. Characterization of the Haptic Actuator*

Figure 7 shows the mode shapes of the haptic actuator computed via modal analysis. The first three mode frequencies were 194.3, 195.3, and 206 Hz, respectively. While the first two modes were related to the transverse motion of the spring, the third mode was the main vibration mode directly related to the electromagnetic excitation (i.e., the vertical oscillator). The solid blue line with a square symbol in Figure 8 shows the simulated acceleration of the actuator in the frequency range of 160–240 Hz. According to the frequency response, the resonance frequency of the actuator was estimated to be approximately 206 Hz, and the acceleration level was approximately 2766 mm/s$^2$.

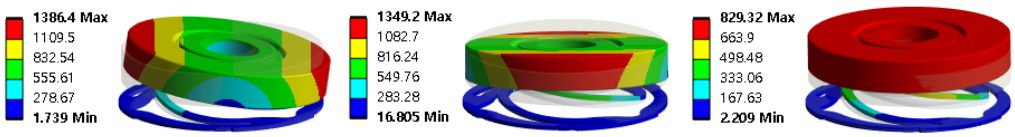


<Mode 1> <Mode 2> <Mode 3>

**Figure 7.** Simulated mode shapes of the haptic actuator.

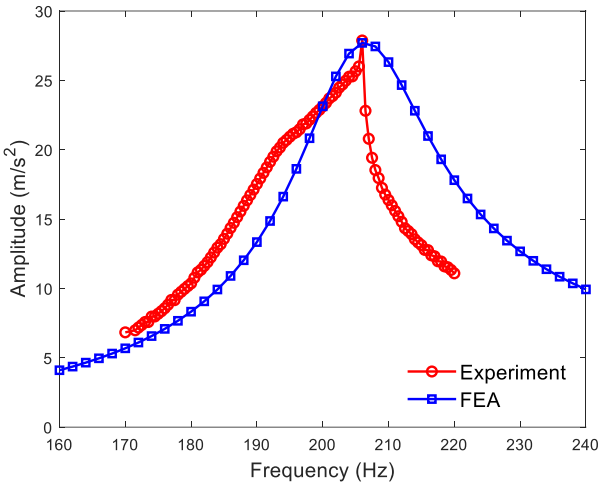


**Figure 8.** Comparison of frequency response functions in the FEA and the experiment.

The test results confirmed the resonance frequency and the corresponding frequency response of the actuator. The solid red line with a circular symbol in Figure 8 shows the acceleration response as a function of frequency, where the maximum peak was found at approximately 206 Hz. The actual acceleration at the resonance was approximately

2786 mm/s$^2$. The resonance frequency in the test was 206 Hz, which is in good agreement with the simulation results. The discrepancy in the acceleration levels between the test and simulation results was less than 1%. To confirm the FE results of the haptic actuator, the actuation condition was applied to the full model of the dial gear shifter (Figure 5).

### *3.2. Vibration Responses and Sensitivity Analysis*

The vibration response of the dial gear shifter was calculated at the surface of the knob using the average acceleration value, as shown in Figure 9. Vibration was generated in the form of a harmonic force using a haptic actuator integrated within the dial gear shifter (Figure 5). For the reference model (i.e., experiment number 1 in Table 3), the acceleration levels at the knob were 3000 mm/s$^2$ on average and 2500 mm/s$^2$ at minimum. To confirm the performance of the baseline model, we conducted FEA for the other test cases. Table 4 lists the vibration responses measured at the knob grip and a comparison of the SNR. Figure 10 shows the sensitivities of each design parameter on the dB scale computed using the SNRs in Table 4. For parameter (A) (i.e., the radius of the knob grip), the condition of 31 mm exhibited the greatest SNR. Regarding the longitudinal length of the knob grip (i.e., (B)), a relatively short length was preferred. According to the sensitivity analysis of parameter (C), it is desirable to remove the side supports to increase the vibration output. Finally, as shown in (D), the knob grip must be attached by bonding rather than by applying screws.

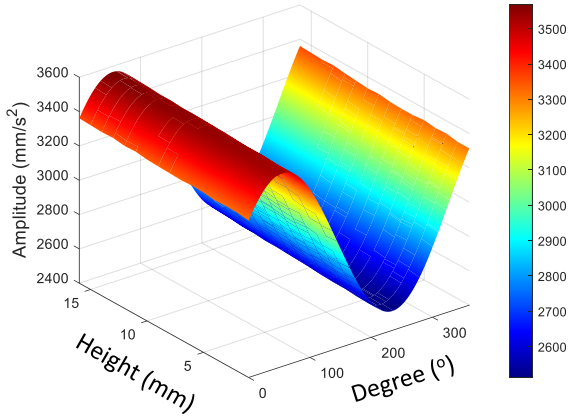


**Figure 9.** Vibration response at the knob grip of the baseline model, observed at the height and the angle of the knob grip.

**Table 4.** Vibration responses for each test case and the SNR.

| No. | Acceleration (mm/s$^2$) | SNR (dB) |
|---|---|---|
| 1 | 3043.2 | 69.667 |
| 2 | 3450.8 | 70.758 |
| 3 | 3399.4 | 70.628 |
| 4 | 3322.9 | 70.430 |
| 5 | 3251.5 | 70.242 |
| 6 | 3698.0 | 71.359 |
| 7 | 3131.8 | 69.916 |
| 8 | 3519.4 | 70.929 |
| 9 | 3436.0 | 70.721 |

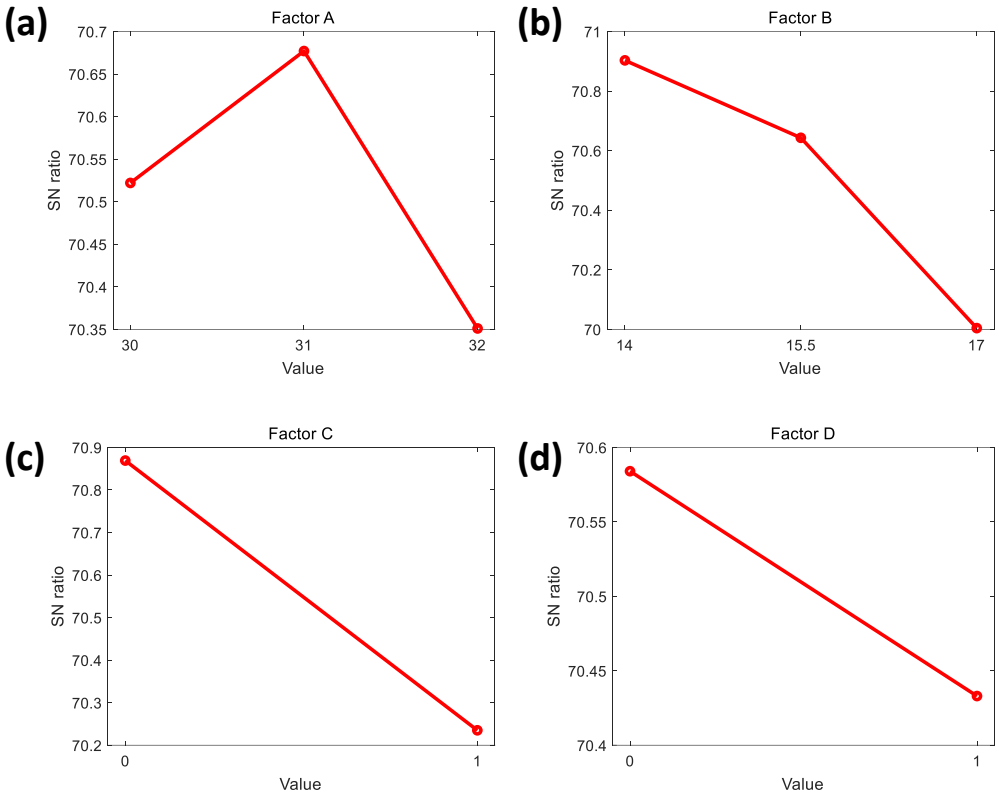


**Figure 10.** Sensitivity analysis of each design parameter for (**a**) the radius of the knob grip, (**b**) the longitudinal length of the knob grip, (**c**) the presence of the side supports, and (**d**) the method of attaching the knob grip.

### *3.3. Optimized Design of the Numerical Model*

Based on the sensitivity analysis results, we determined the optimal design parameters for enhancing the vibration response at the knob grip of a dial gear shifter. The highest SNR was observed when (A) = 31 mm, (B) = 14 mm, (C) = 0, and (D) = 0. However, we found that parameter (B) still had room for further reduction because the SNR tended to increase with a smaller knob grip length. Therefore, 13 mm was selected for parameter (B) in the optimal design (Figure 11). Figure 12 shows the vibration response of the numerical model after incorporating the optimal design parameters. The optimized model exhibited a relatively large acceleration value of 3800 mm/s$^2$, showing a significant increase in the vibration response at the knob grip of more than 26.7%.

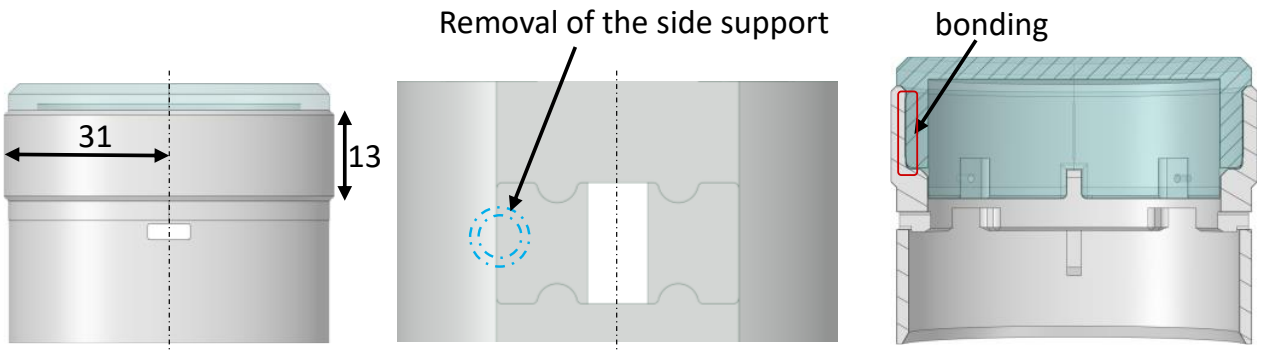


**Figure 11.** Optimized design of dial gear shifter to potentiate the level of haptic vibration.

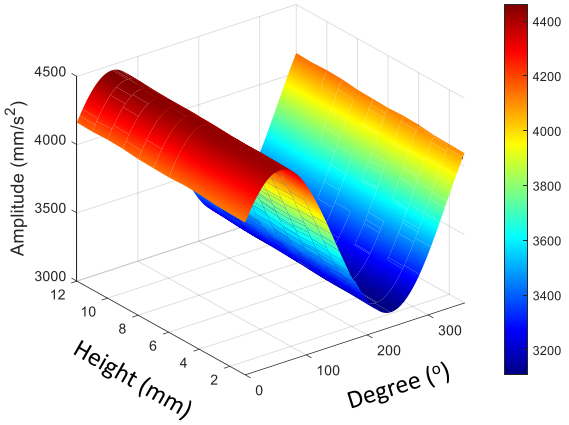


**Figure 12.** Vibration response at the knob grip of the design-optimized model, observed at the height and the angle of the knob grip.

### *3.4. Discussion*

In this study, we investigated the design optimization of a dial gear shifter module integrated with a haptic actuator through numerical analyses. First, we accurately estimated the forcing condition of the haptic actuator by comparing the FEA and experiment results (Figure 8). A dial gear shifter is installed inside a vehicle and operates only under specific conditions. Therefore, this study did not incorporate the temperature effects or long-term operation issues in the numerical analysis. The comparison between the frequency response functions of the FEA and the experiment results revealed slight differences, as shown in Figure 8. For example, the frequency response in the experiment was asymmetric with respect to the resonance frequency, whereas the simulated result appeared relatively symmetric, and there was no significant variation in the frequency or vibration level. The discrepancy in the shape of the frequency response could be attributed to the nonlinearity in the actual haptic actuator. Although the haptic actuator had a rubber damper inside the oscillator, it was difficult to realize the numerical modeling of the nonlinear contact through harmonic analysis using an FE model. Therefore, rather than including the damper in the numerical model, we tuned the model damping using the experiment results. Meanwhile, we hypothesized that the nonlinear effects caused by frequency coupling and the damper would be marginal. However, since we compared the vibration characteristics of each design parameter relatively, the linearized model could still compute the optimal design parameters at the single-frequency condition of the actuator integrated into the gear shifter.

Following the vibration analysis of the haptic actuator, we constructed an FE model of the dial gear shifter. The minimum acceleration at the knob grip was estimated to be approximately 2500 mm/s$^2$ in the baseline model (Figure 9). However, the acceleration level in the baseline model was not sufficient to realize the actual tactile feeling of the user; this is based on past research indicating that the minimum threshold at the given frequency range should be at least 2500 mm/s$^2$ [31]. Therefore, we conducted a design optimization of the numerical model of a dial gear shifter with the aid of an L9 orthogonal array and a sensitivity analysis (Table 4 and Figure 10). The span of the design parameters in the optimizing process was from 1 to 1.5 mm in 0.5 mm intervals. The parameter interval was greater than the typical manufacturing tolerances of plastic products (~0.1 mm). Therefore, the minor discrepancy caused by the production process would be negligible. The optimal combination of design parameters significantly increased the resulting vibration level by 26.7% compared with that of the baseline model (Figure 12). The minimum and average acceleration levels at the knob exceeded the known threshold by >20%. Hence, it was expected that the haptic actuator would operate at a relatively lower voltage input compared to the baseline model, thereby saving electrical energy. Lastly, we must mention that hand-grabbing effects were not addressed in this paper as we assumed that the force exerted by two or three fingers on the knob would not be too large. Moreover, it was not a

simple problem to define the hand-grabbing force for average people. Though a multi-step analysis (i.e., static analysis and the following harmonic analysis) would provide a more realistic result by including such effects, an analysis addressing the hand-grabbing effect would be an interesting research topic.

As such, numerical analyses could predict the vibration responses at the knob grip of a dial gear shifter through multiple trial models without requiring actual product fabrication. Furthermore, the optimal design can confirm the vibration characteristics of a product without conducting actual experiments. The research results will provide a technical background for the fabrication of an actual dial gear shifter with a relatively high sensitivity to the haptic response.

## 4. Conclusions

This study investigated the design optimization of a dial gear shifter using a haptic actuator. The numerical model of the haptic actuator exhibited a reliable agreement (within 1% of the resonance frequency and vibration level) with the actual model. Following the validation of the actuator model performance, we conducted an FEA to ensure that the product could provide a sufficient level of haptic feeling to users. Because the baseline model was not able to generate sufficiently high acceleration at the hand grip, we performed a design optimization process. Four design parameters were considered, and the optimal design of the dial gear shifter was determined via a sensitivity analysis such that it exhibited a relatively high level of vibration (>25%). It was noticeable that an enhancement of over 27% in the vibration level could be achieved with a marginal change of the design parameters. It is thus meaningful to determine the optimal design out of the nine design candidates using numerical analyses without fabricating an actual product. In future work, we will demonstrate the performance of haptic actuation in a dial gear shifter using a real prototype and human assessments.

**Author Contributions:** Conceptualization, H.K.; Methodology, H.E. and C.K.; Software, J.C.; Formal analysis, J.W. and J.C.; Investigation, H.K; Resources, K.K. and H.K.; Data curation, J.W., H.E. and C.K.; Writing—original draft, J.W.; Writing—review & editing, K.K. and H.K.; Project administration, H.K.; Funding acquisition, K.K. and H.K. All authors have read and agreed to the published version of the manuscript.

**Funding:** This work was supported by the Technology Innovation Program (or Industrial Strategic Technology Development Program-the Technology Innovation Program) (20026372, Smart safety-based SCU and e-Shift module system integration technology and demonstration technology development) funded By the Ministry of Trade, Industry & Energy (MOTIE, Korea). This work was supported in part by an INHA UNIVERSITY research grant (No. 71354-1).

**Institutional Review Board Statement:** Not applicable.

**Informed Consent Statement:** Not applicable.

**Data Availability Statement:** The data presented in this study are available on request from the corresponding author. The data is not publicly available due to privacy.

**Acknowledgments:** The authors would like to acknowledge Kaphyun Cho at Sanil Co., Ltd. (Incheon, S. Korea) for providing test samples of the haptic actuators and sharing the information on the frequency response of the actuator.

**Conflicts of Interest:** Authors Kinyung Ko and Heesoo Eom were employed by the company LS Automotive Technologies Co., Ltd. The remaining authors declare that the research was conducted in the absence of any commercial or financial relationships that could be construed as a potential conflict of interest.

## References

1. Mourtzis, D.; Angelopoulos, J.; Panopoulos, N. The future of the human–machine interface (HMI) in society 5.0. *Future Internet* **2023**, *15*, 162. [CrossRef]
2. Bengler, K.; Rettenmaier, M.; Fritz, N.; Feierle, A. From HMI to HMIs: Towards an HMI framework for automated driving. *Information* **2020**, *11*, 61. [CrossRef]

3. Naujoks, F.; Hergeth, S.; Wiedemann, K.; Schömig, N.; Forster, Y.; Keinath, A. Test procedure for evaluating the human–machine interface of vehicles with automated driving systems. *Traffic Inj. Prev.* **2019**, *20*, 146–151. [CrossRef]
4. Jansen, B.J. The graphical user interface. *ACM SIGCHI Bull.* **1998**, *30*, 22–26. [CrossRef]
5. Walch, M.; Lange, K.; Baumann, M.; Weber, M. Autonomous driving: Investigating the feasibility of car-driver handover assistance. In Proceedings of the 7th International Conference on Automotive User Interfaces and Interactive Vehicular Applications, Nottingham, UK, 1–3 September 2015.
6. Cornelio, P.; Velasco, C.; Obrist, M. Multisensory integration as per technological advances: A review. *Front. Neurosci.* **2021**, *15*, 652611. [CrossRef]
7. Albustanji, R.N.; Elmanaseer, S.; Alkhatib, A.A. Robotics: Five senses plus one—An overview. *Robotics* **2023**, *12*, 68. [CrossRef]
8. Maggioni, E.; Cobden, R.; Dmitrenko, D.; Hornbæk, K.; Obrist, M. SMELL SPACE: Mapping out the olfactory design space for novel interactions. *ACM Trans. Comput. Hum. Interact.* **2020**, *27*, 1–26. [CrossRef]
9. Ratcliffe, M. Touch and situatedness. *Int. J. Philos. Stud.* **2008**, *16*, 299–322. [CrossRef]
10. Maereg, A.T.; Nagar, A.; Reid, D.; Secco, E.L. Wearable vibrotactile haptic device for stiffness discrimination during virtual interactions. *Front. Robot. AI* **2017**, *4*, 42. [CrossRef]
11. Katzschmann, R.K.; Araki, B.; Rus, D. Safe local navigation for visually impaired users with a time-of-flight and haptic feedback device. *IEEE Trans. Neural Syst. Rehabil. Eng.* **2018**, *26*, 583–593. [CrossRef]
12. Balachandran, A.; Brown, M.; Erlien, S.M.; Gerdes, J.C. Predictive haptic feedback for obstacle avoidance based on model predictive control. *IEEE Trans. Autom. Sci. Eng.* **2015**, *13*, 26–31. [CrossRef]
13. Chang, W.; Hwang, W.; Ji, Y.G. Haptic seat interfaces for driver information and warning systems. *Int. J. Hum.-Comput. Int.* **2011**, *27*, 1119–1132. [CrossRef]
14. Petermeijer, S.M.; Abbink, D.A.; Mulder, M.; De Winter, J.C. The effect of haptic support systems on driver performance: A literature survey. *IEEE Trans. Haptics* **2015**, *8*, 467–479. [CrossRef]
15. Chun, J.; Han, S.H.; Park, G.; Seo, J.; Choi, S. Evaluation of vibrotactile feedback for forward collision warning on the steering wheel and seatbelt. *Int. J. Ind. Ergon.* **2012**, *42*, 443–448. [CrossRef]
16. Wang, Z.; Zheng, R.; Kaizuka, T.; Shimono, K.; Nakano, K. The effect of a haptic guidance steering system on fatigue-related driver behavior. *IEEE Trans. Hum.-Mach. Syst.* **2017**, *47*, 741–748. [CrossRef]
17. Gaffary, Y.; Lécuyer, A. The use of haptic and tactile information in the car to improve driving safety: A review of current technologies. *Front. ICT* **2018**, *5*, 5. [CrossRef]
18. Beruscha, F.; Krautter, W.; Lahmer, A.; Pauly, M. An evaluation of the influence of haptic feedback on gaze behavior during in-car interaction with touch screens. In Proceedings of the IEEE World Haptics Conference, Munich, Germany, 6–9 June 2017.
19. Hirokawa, M.; Uesugi, N.; Furugori, S.; Kitagawa, T.; Suzuki, K. Effect of haptic assistance on learning vehicle reverse parking skills. *IEEE Trans. Haptics* **2014**, *7*, 334–344. [CrossRef] [PubMed]
20. Hwang, S.; Ryu, J.H. The haptic steering wheel: Vibro-tactile based navigation for the driving environment. In Proceedings of the 8th IEEE International Conference on Pervasive Computing and Communications Workshops, Mannheim, Germany, 29 March–2 April 2010.
21. De Rosario, H.; Louredo, M.; Díaz, I.; Soler, A.; Gil, J.J.; Solaz, J.S.; Jornet, J. Efficacy and feeling of a vibrotactile Frontal Collision Warning implemented in a haptic pedal. *Transp. Res. F Traffic Psychol. Behav.* **2010**, *13*, 80–91. [CrossRef]
22. De Nijs, S.Y.; Mulder, M.; Abbink, D.A. The value of haptic feedback in lane keeping. In Proceedings of the IEEE International Conference on Systems, Man, and Cybernetics, San Diego, CA, USA, 5–8 October 2014.
23. Shakeri, G.; Brewster, S.A.; Williamson, J.; Ng, A. Evaluating haptic feedback on a steering wheel in a simulated driving scenario. In Proceedings of the CHI Conference Extended Abstracts on Human Factors in Computing Systems, San Jose, CA, USA, 7–12 May 2016.
24. Fitch, G.M.; Hankey, J.M.; Kleiner, B.M.; Dingus, T.A. Driver comprehension of multiple haptic seat alerts intended for use in an integrated collision avoidance system. *Transp. Res. F Traffic Psychol. Behav.* **2011**, *14*, 278–290. [CrossRef]
25. Breitschaft, S.J.; Pastukhov, A.; Carbon, C.C. Where's my button? Evaluating the user experience of surface haptics in featureless automotive user interfaces. *IEEE Trans. Haptics* **2021**, *15*, 292–303. [CrossRef]
26. Abbink, D.A.; Mulder, M.; Van der Helm, F.C.; Mulder, M.; Boer, E.R. Measuring neuromuscular control dynamics during car following with continuous haptic feedback. *IEEE Trans. Syst. Man. Cybern. B Cybern.* **2011**, *41*, 1239–1249. [CrossRef]
27. Xu, X.; Dong, P.; Liu, Y.; Zhang, H. Progress in automotive transmission technology. *Automot. Innov.* **2018**, *1*, 187–210. [CrossRef]
28. Pyo, D.; Yang, T.H.; Ryu, S.; Kwon, D.S. Novel linear impact-resonant actuator for mobile applications. *Sens. Actuators A Phys.* **2015**, *233*, 460–471. [CrossRef]
29. Jackson, J.D. *Classical Electrodynamics*, 3rd ed.; Wiley: Hoboken, NJ, USA, 1999; pp. 237–242.
30. Karna, S.K.; Sahai, R. An overview on Taguchi method. *Int. J. Math. Sci.* **2012**, *1*, 1–7.
31. Howe, R.D.; Cutkosky, M.R. Sensing skin acceleration for slip and texture perception. In Proceedings of the ICRA, Scottsdale, AZ, USA, 14–19 May 1989.


**Disclaimer/Publisher's Note:** The statements, opinions and data contained in all publications are solely those of the individual author(s) and contributor(s) and not of MDPI and/or the editor(s). MDPI and/or the editor(s) disclaim responsibility for any injury to people or property resulting from any ideas, methods, instructions or products referred to in the content.